Investigation of Potential Bare Ground Modeling Techniques using Multispectal Satellite Imagery

Keith T. Weber, GISP, GIS Director, Idaho State University, GIS Training and Research Center, Idaho State University, Pocatello, Idaho, 83209-8104, USA (webekeit@isu.edu)

Nancy F. Glenn, Research Associate Professor, Idaho State University, Dept. of Geosciences, 322 E. Front St., Suite 240, Boise, Idaho 83702

Jacob Tibbitts, Idaho State University, GIS Training and Research Center, 921 S. 8th Ave., Stop 8104, Pocatello, Idaho 83209-8104

ABSTRACT

Bare ground exposure is an important indicator of rangeland health in semi-arid ecosystems. As such, numerous studies have attempted to detect bare ground exposure using a variety of remote sensing platforms and image processing techniques with varying levels of success. This paper describes a study that investigates the potential of various techniques, indices, and algorithms (NDVI, Angle indices, SMA, and SAM) to accurately detect bare ground exposure within semi-arid rangelands of southeastern Idaho. Results indicate that while each technique may function well where bare ground is common ($\geq$50%), none of the techniques tested appear suitable in areas where bare ground exposure rarely exceeds 35% save for the Angle at near infrared (ANIR index which may be able to detect bare ground with as little as 10% exposure.

KEYWORDS: GIS, remote sensing, bare ground exposure

INTRODUCTION

The degree of bare ground exposure has a major influence on rangeland ecological function (Whitford et al. 1998, Pyke et al. 2002, O'Brien et al. 2003, Hunt et al. 2003, Booth and Tueller 2003) and when determining rangeland health, bare ground exposure is frequently a primary indicator. In a joint collaboration between the USDI-BLM, USGS, USDA-NRCS, and USDA-ARS, 17 indicators of rangeland health were identified (Pellant 1996, Pyke et al 2002) and a subsequent USDA-ARS study (O'Brien et al. 2003) noted that 11 of the 17 indicators and a majority of indicators used by others (Williams and Kepner 2002) dealt with bare ground exposure. The degree of bare ground exposure affects the ecological attributes of soil/site stability, hydrological function, and biotic integrity (Savory 1999, Booth and Tueller 2003) and has been linked with both decreased vegetation production and biodiversity (Daubenmire 1959), increased soil erosion (Morgan 1986, Okin and Reheis 2001), and increased water run-off (Kincaid and Williams 1966, Branson and Shown 1970). Furthermore, bare ground contributes to increased amounts of particulate matter suspended in the air, through dust storms, that can consist of herbicides, pesticides, and large particulates that have detrimental health effects on humans and the environment (DeFries and Townshend 1994, Griffin et al. 2001, Okin and Reheis 2001). Since the degree of bare ground exposure is such an important indicator or rangeland health, accurate bare ground modeling provides important data to objectively assess rangelands (Whitford et al. 1998, O'Brien et al. 2000, Booth and Tueller 2003, Hunt et al. 2003) and improve the management and stewardship of these important ecosystems.

Remote sensing provides an opportunity to monitor rangelands, and specifically bare NAground exposure, at landscape scales and continuous extents with multi-temporal capabilities (Booth and Tueller 2003). Although previous studies recognize the importance of bare ground detection and modeling--and acknowledge the need for bare ground monitoring--there are a lack of studies focusing solely on bare ground detection thresholds, limitations, and reliability using remote sensing (Booth and Tueller 2003, Palmer and Fortescue 2003, Washington-Allen et al. 2006, Gokhale and Weber 2006). One difficulty in remote sensing of rangelands is the frequency of spectral mixing present within each pixel (Weber 2006).

This study investigates the suitability and limitations of bare ground detection with multispectral remote sensing data. The hypothesis of this study is that bare ground's unique spectral signal in the visible to shortwave infrared portions of the electromagnetic spectrum coupled with Spectral Mixture Analysis (SMA) and Spectral Angle Mapper (SAM) can be used to accurately discriminate and quantify bare ground exposure where bare ground is relatively rare (< 50% exposure). This hypothesis is tested through development of SMA and SAM techniques to discriminate bare ground using Satellite Pour l'Observation de la Terre 5 (SPOT 5) and Advanced Spaceborne Thermal Emission and Reflection Radiometer (ASTER) multispectral remote sensing data and various accuracy assessment techniques.

METHODS

Study Area

The O'Neal Ecological Reserve, is located in sagebrush-steppe rangelands of southeastern Idaho, and is approximately 30 km south of Pocatello (Figure 1). This 50 ha site, located along the Portneuf River, contains sagebrush-steppe upland areas upon lava benches. Adjacent to the O'Neal Ecological Reserve is a USDI BLM grazing allotment called the Rocks. The soils within the study area are a McCarey-McCarey Variant complex that is shallow and well drained. The O'Neal study area averages <0.38 m of precipitation annually with the majority falling as winter snow. The O'Neal study area is relatively flat with little relief and has an elevation of approximately 1400 m (1401-1430 m). The dominant plant species is Mountain Big Sagebrush (*Artemesia tridentata*) with various native and non-native grasses including bluebunch wheatgrass (*Pseudoroegneria spicata)*, Indian rice grass (*Oryzopsis hymenoides*), and Needle-and-Thread (*Stipa comata*).

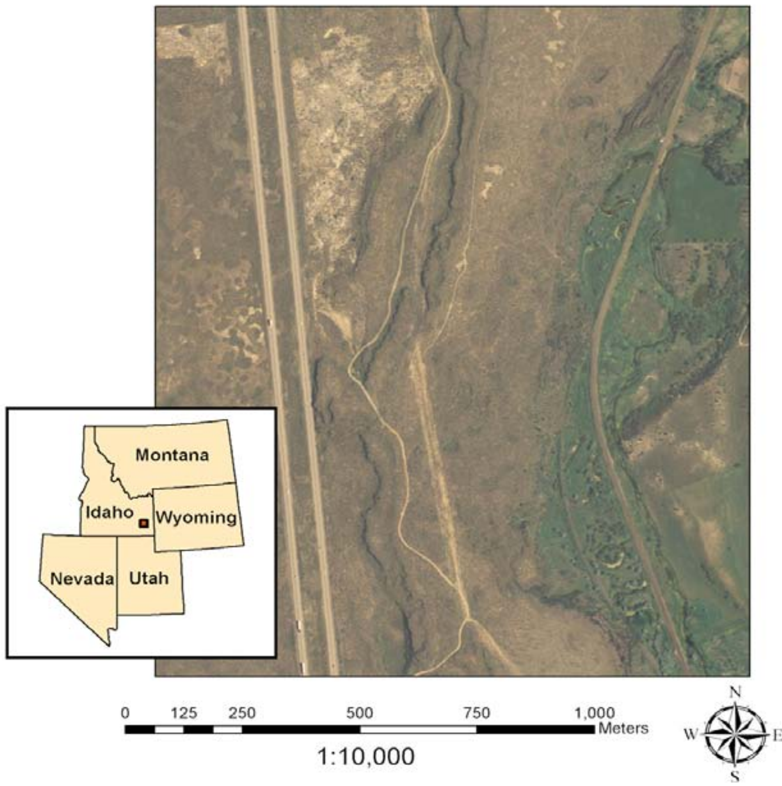

Figure 1. Location and general characteristics of the O'Neal Ecological Reserve study site.

Field Data Collection

Sample points (*n*=150) were randomly generated using Hawth's tools in ESRI's ArcMap GIS software. Field data were collected between 18 June 2007 and 16 July 2007 and due to technical difficulties, three sample points were not collected, leaving 147 for subsequent analysis (Figure 3). Sample points were navigated to using a Trimble GeoXH GPS receiver (+/- 0.30 m @ 95% CI after post-processing using Trimble H-star technology). Once at the pre-designated sample point, a 10 m x 10 m plot was centered over each point with the edges of the plot aligned in the cardinal directions. Percent cover estimates were made for each 100 m^2 plot using the point-intercept method (Herrick, et al 2005). Two 10 m line transects were positioned perpendicular to each other and crossing at plot center (i.e., the 5.0m mark of each line transect). Observations of cover type were made every 0.20 m along each 10 m transect, beginning at 0.10 m and ending at 9.90 m (n = 50 points for each line and n = 100 points for each plot). The first layer of canopy observed from nadir at each observation point was recorded as either: bare ground, rock ($\geq$75 mm), litter, dead herbaceous material, standing dead woody material, live herbaceous species, or live shrub. Rock that was < 75 mm was recorded as bare ground. While the focus of this study was the detection of bare ground, ground-cover types other than bare ground were recorded to better understand the spectral dynamics within each pixel.

Image Acquisition and Pre-processing

Multispectral satellite imagery was collected over the study area on June 17th and June 29th, 2007. This range of dates temporally coincided with ground sampling efforts during that year. SPOT 5 was acquired on June 29th which collects data in four spectral bands from the visible (545nm band center) through the near-infrared (NIR, 840nm band center) and short-wave infrared (SWIR, 1665nm band center) regions of the electromagnetic spectrum. The green, red, and NIR bands have a spatial resolution of 10 m while the SWIR band has a spatial resolution of 20 m (note: the SWIR band was resampled by SPOT image corporation to 10 m prior to delivery). ASTER imagery was acquired on June 17th which collects data in 14 spectral bands from the visible (560nm band center) to the thermal infrared (TIR, 11300nm band center for band 14). The spatial resolution of ASTER images vary by band: 15 m for all (3) visible and NIR bands, 30 m for all (6) SWIR bands, and 90 m for all (5) TIR bands. The SWIR bands were resampled to 15 m to match the resolution of the VNIR bands using ESRI's ArcGIS software and nearest neighbor resampling algorithm. The TIR bands were not used in this study.

SPOT 5 and ASTER data were delivered as level 1A and 1B (radiometrically corrected), respectively. SPOT 5 data were processed to reflectance by performing an atmospheric correction using the Cos(t) image-based absolute correction method (Chavez 1988) in Idrisi Andes software (Clark Labs, Worcester, MA). ASTER data were converted to radiance at the sensor using published conversion coefficients (Abrams et al. 1999). The radiance data was then converted to top of atmosphere (TOA) reflectance (using mean solar exoatmospheric irradiance (ESUN) for each band as reported by Thome et al. (2001) and the standard Landsat TOA equation from the Landsat 7 Science Data Users Handbook (Williams 1998). All imagery was geo-rectified to the study area and co-registered using ESRI's ArcMap and national agricultural imagery program aerial photography (2004) with 1 mpp resolution as well as high resolution aerial imagery (2005) with 0.05 mpp resolution with an absolute accuracy of +/- 0.015m based upon surveyed ground control points. Nearest neighbor resampling was used in all cases and the RMSE was 3.15 and 4.44 for the SPOT and ASTER imagery, respectively.

Image Processing

<u>Normalized Difference Vegetation Index</u>

The Normalized Difference Vegetation Index (NDVI) was calculated using both SPOT and ASTER datasets and the respective NDVI results were regressed against *in situ* bare ground measurements to determine the level of agreement between known bare ground exposure and vegetation index values. Vegetation indices have been previously correlated to bare ground exposure in semi-arid environments (McMurtrey et al. 1993) suggesting this simple technique has merit and for this reason was included in this study.

<u>Angle Index</u>

Roberts et al. (1993) noted that non-photosynthetic vegetation (NPV; i.e., litter) and bare ground may not be separable using multispectral sensors because of cellulose absorption within the bandwidths employed by multispectral sensors (van Leeuwen and Huete 1996). However, recent developments of two angle indices, the Angle at Near-Infrared (ANIR) and the Shortwave Angle Slope Index (SASI) offer some promise for discriminating NPV from soil by exploiting the information contained within multispectral imagery and uncovering band relationships between bands instead of relying solely upon reflectance data (Khanna et al. 2007). The ANIR index was calculated using SPOT 5 data following methods described in

Khanna et al. (2007). SASI could not be calculated with SPOT 5 data as its SWIR band does not extend out to 2200nm as required for this index. However, the SASI was determined using ASTER imagery. Calculation of these indices was performed using ESRI's ArcMap and resulting values at each field sample location were extracted to a database table for statistical analysis and comparison with ground truth values.

Spectral Mixture Analysis

Using RSI's ENVI, the Minimum Noise Fraction (MNF) transformation was performed using SPOT 5 imagery as a data reduction technique to uncover data dimensionality and segregate noise in the data (Boardman and Kruse 1994). Since MNF bands were required for further image analysis using spectral mixture analysis, this step was used to determine if all MNF bands (based upon dimensionality) were required for future processing and analysis.

In order to preserve full data dimensionality, four output MNF layers were used to match the number of bands in the SPOT 5 imagery. The MNF transformation used the shift difference method (Ifarraguerri and Chang 2000) for calculation of noise statistics. This method uses local pixel variance to estimate noise. The results of the MNF transformation were then used for additional spectral mixture analysis (SMA) processing with the next step being an investigation of pixel purity.

By randomly and repeatedly projecting scatter plots of the four MNF bands in n-Dimensions (in this case 4-dimensions), the pixel purity index (PPI) counts the number of times that each pixel is marked as a possible pure end-member at the extreme end of each projected vector. A threshold value of 3.0 was chosen to specify the minimum number of pixels that were marked at the ends of each projected vector. The number of iterations performed was 25,000 and a PPI image was created from this process in which an individual pixel's value represented the number of times that pixel was chosen as a possible pure end-member pixel. The maximum number of pixels used by the n-Dimensional Visualizer (n-DV) was set at 10,000. This allowed for visualization of the best PPI pixels but did not encumber the visualization process with too many pixels.

SMA or Linear Spectral Un-mixing assumes a mixed pixel can be modeled as a linear combination of spectrally pure end-members. To determine the composition of a mixed pixel requires the pixel to be broken down into its fractional proportion relative to each target end-member (Roberts et al. 1993, Settle and Drake 1993, Adams et al. 1995). Based upon these assumptions, the bare ground end-members derived from the PPI and n-DV were used to partially un-mix the SPOT 5 imagery into a fractional bare ground exposure layer. The SMA results were then regressed against ground truth data for evaluation.

Spectral Angle Mapper (SAM) classifies imagery by calculating the angle between each pixel to the end-member spectral vectors in n-dimensional space (where n = number of bands). Smaller angles represent better matches with the target end-member spectra (Kruse et al. 1993) and the best match is considered the most probable identification of that pixel. The bare ground end-members derived from PPI and n-DV were used for SAM classification. The results of this classification were regressed against ground truth data for evaluation.

Error Assessment

Since no classification was performed using NDVI, the accuracy of this approach was estimated using linear regression analysis to calculate correlation between NDVI values and known bare ground exposure.

The bare ground models derived from angle indices produced a classified layer of bare ground/non-bare ground by applying the threshold values described by Khanna et al. 2007. Producer accuracy was then calculated from the classified model.

To determine the ability of both SMA and SAM classifiers to accurately detect bare ground exposure in semi-arid rangelands using multispectral imagery, linear regression analyses were evaluated with particular attention given to the resulting coefficient of determination (R^2).

RESULTS AND DISCUSSION

Field data collection

Only ten percent of all 2007 field samples (n = 14) had >50 % exposed bare ground while 77% of these samples (n = 113) had bare ground exposure <=35 %. Based upon the research presented by others (Booth and Tueller 2003, Palmer and Fortescue 2003, Washington-Allen et al. 2006, Gokhale and Weber 2006) the majority of field training sites collected for this study had target levels below the suggested minimum threshold for reliable detection. However, the previous studies did not apply spectral un-mixing techniques (e.g., Gokhale and Weber [2006] used the maximum-likelihood classifier) which may be capable of improving target detection threshold levels.

NDVI

NDVI has poor correlation with bare ground exposure as the coefficient of determination (R^2) was only 0.187. The use of NDVI to classify bare ground was not explored further.

Angle Indices

As the amount of bare ground exposure increases, both ANIR and SASI indices were expected to increase (Khanna et al 2007). In this study, the ANIR values derived from SPOT5 imagery (2.91 to 3.13) follow this trend as do the ANIR (2.03-2.57) and SASI (-0.085 to 0.017) values derived from ASTER imagery, although only marginally in all cases. Khanna et al (2007) classified every pixel with an ANIR value of 2.4 or higher and a SASI value of -0.01 and higher as "soil, residue and low-leaf area index vegetation." Using SPOT5 ANIR values classified all ground truth sites (n=147) as bare ground sites including those where no bare ground was found in the field (n=15, or approximately 10% of all sample sites). Using ASTER ANIR values resulted in seven sites known to have no bare ground exposure classified as a bare ground site, while the majority of known non-bare ground sites were correctly classified (53%; Table 1). It is interesting that when bare ground exposure exceeds 10%, the ASTER ANIR classification improved steadily.

Table 1. Distribution of classified pixels in the bare ground model produced using the ANIR index (ASTER imagery) and threshold values suggested by Khanna et al (2007)

	Known bare ground exposure				
	0	**10**	**20**	**30**	**40**
Bare ground class	0.47	0.76	0.80	0.50 a	0.50 a
Non-bare ground class	0.53	0.24	0.20	0.50 a	0.50 a

a. These results based upon sample size of one.

Similar to the SPOT5 ANIR classification, the classification using ASTER SASI values classified all (n=147) ground truth sites as a bare ground area. As a result, both SPOT5 ANIR and ASTER SASI classifications were considered unreliable as they grossly overestimated bare ground exposure at the O'Neal study area.

Spectral Mixture Analysis

Visual examination of the four resulting MNF bands did not demonstrate noticeable degradation of image quality for any of the MNF bands suggesting that a spatial coherence threshold was not reached (Figure 2) with either the multispectral SPOT 5 or ASTER imagery and these data could not be further reduced. Therefore, all four MNF bands were selected as input bands for further image processing.

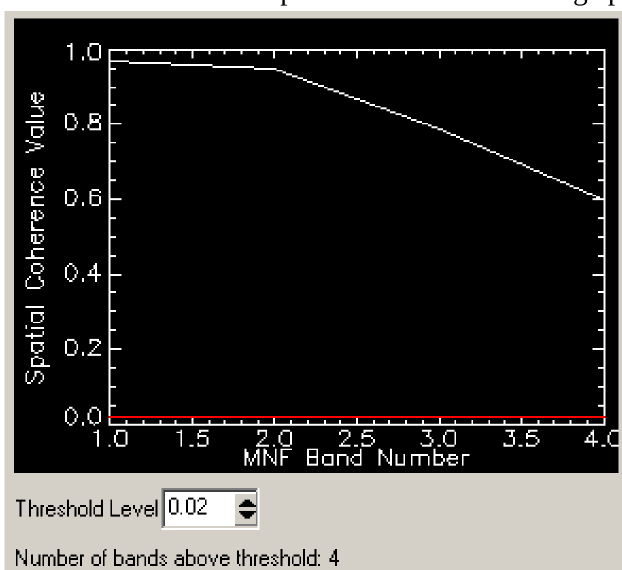

Figure 2. Example of spatial coherence threshold testing with ENVI software (SPOT 5 data is shown in this illustration).

End-member Selection

The results from pixel purity index (PPI) analysis were used in the n-Dimensional Visualizer (n-DV) to retrieve end-members. The n-DV plots the pixels as a scatter plot (pixel cloud) that can be viewed and rotated in minimum noise fraction (MNF) space with the number of dimensions being equal to the number of MNF bands used (e.g., four in the case of SPOT imagery). The purest pixels plot at the corners of the scatter plot and form candidate end-members. However, none of the candidate end-member pixels coincided with areas where field data was available and as a result, these candidate end-members could not be validated directly. To validate these pixels as bare ground end-members, the spectral signatures of the candidate end-members were extracted and compared to reflectance signatures of known bare ground pixels within the study area. As a result, the spectral signatures for the candidate end-members were accepted and a spectral mixture analysis classification completed.

Regressions between spectral mixture analysis models of bare ground exposure and known percent bare ground revealed weak coefficients of determination when using either SPOT (R^2 = 0.243) or ASTER imagery (R^2 = 0.179) (Figures 3 and 4)

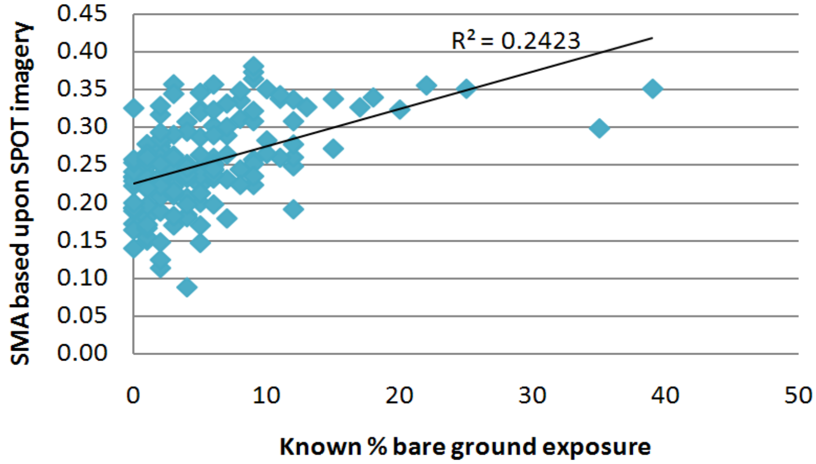

Figure 3. Regression between SMA scores for bare ground training sites and known bare ground exposure using SPOT satellite imagery.

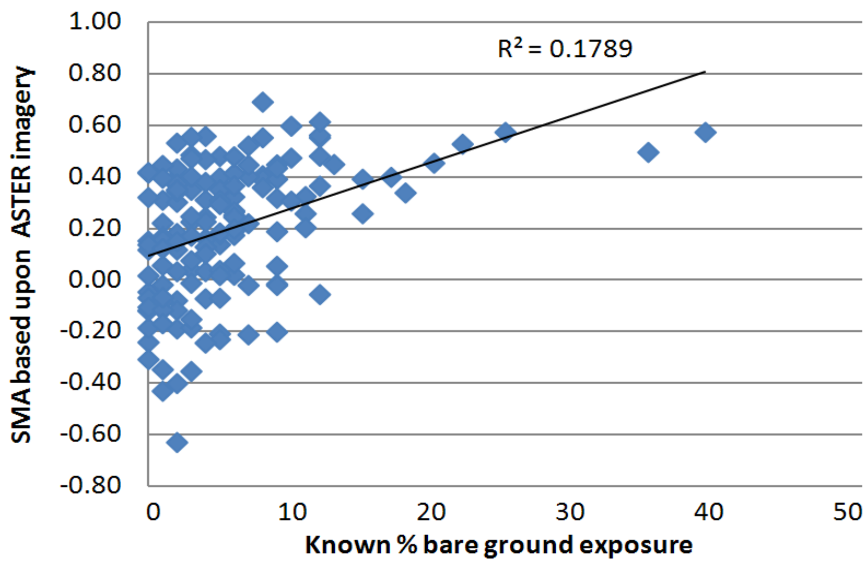

Figure 4. Regression between SMA scores for bare ground training sites and known bare ground exposure using ASTER satellite imagery.

Spectral Angle Mapper

The resulting relationship between SAM scores of bare ground and known bare ground exposure were very low (R^2 = 0.133). No further exploration into the use of SAM was conducted (figure 5).

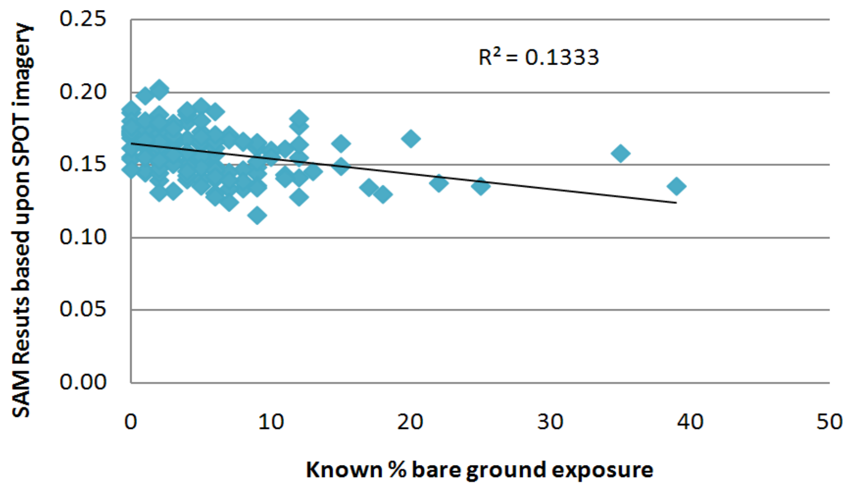

Figure 5. Regression between SAM scores for bare ground training sites and known bare ground exposure using SPOT satellite imagery.

CONCLUSIONS

This study provides an exploration into the potential of various indices and sub-pixel analyses to detect and reliably classify bare ground exposure in semi-arid rangelands using two common multispectral platforms (SPOT 5 and ASTER), where bare ground is relatively rare (<35%). The results of these explorations suggest that none of the techniques tested (NDVI, SASI, SMA, and SAM) have the potential to provide an accurate model of bare ground save for the ANIR index.

The ANIR index was calculated using ASTER imagery (SPOT 5 imagery cannot support this index) and results suggest that bare ground may be detectable at levels as low as 10% exposure. Further research is required to verify this possibility.

ACKNOWLEDGEMENTS

This study was made possible by a grant from the National Aeronautics and Space Administration Goddard Space Flight Center (NNG06GD82G). ISU would also like to acknowledge the Idaho Delegation for their assistance in obtaining this grant.

LITERATURE CITED

Abrams, M., S. Hook, and B. Ramachandran. 1999. ASTER User Handbook, Version 2. Jet Propulsion Laboratory/California Institute of Technology. 135 pp. URL = http://asterweb.jpl.nasa.gov/content/03_data/04_Documents/aster_user_guide_v2.pdf visited 3-Mar-2009

Adams J. B., D. E. Sabol, V. Kapos, R. A. Filho, D. A. Roberts, M. O. Smith, and A. R. Gillespie, 1995: Classification of Multispectral Images Based on Fraction Endmembers: Application to Land-Cover Change in the Brazilian Amazon. Remote Sensing of Environment 52:137–154

Boardman, J.W. 1998. Leveraging the High Dimensionality of AVIRIS Data for Improved Subpixel Target Unmixing and Rejection of False Positives: Mixture Tuned Matched Filtering. In Proceedings of the 7th Annual JPL Airborne Geoscience Workshop, JPL Publication 97-1, Pasadena, CA 55 pp.

Boardman, J. W., and F.A. Kruse, 1994. Automated Spectral Analysis: A Geological Example using AVIRIS Data, Northern Grapevine Mountains, Nevada. in Proceedings, Tenth Thematic Conference, Geologic Remote Sensing, 9-12 May 1994, San Antonio, Texas, p. I-407 - I-418

Booth, D.T. and P.T. Tueller. 2003. Rangeland Monitoring Using Remote Sensing. Arid Land Research and Management 17: 455-467

Branson, F. A. and L. M. Shown. 1970. Plant Cover, Runoff, and Sediment Yield Relationships in Mancos Shale in Western Colorado. Water Resource Res. 6:783-790

Chavez, P. S. 1988. An Improved Dark-Object Subtraction Technique for Atmospheric Scattering Correction of Multispectral Data. Remote Sensing of Environment. 24:459-479

Daubenmire, R. 1959. A Canopy-coverage Method of Vegetational Analysis. Northwest Science 33:43-64.

DeFries, R. S., and J. R. G. Townshend. 1994. NDVI-derived Land Cover Classification at a Global Scale. International Journal of Remote Sensing 15: 3567–3586.

Gokhale, B. and K. T. Weber. 2006. Rangeland Health Modeling with Quickbird Imagery. Pages 3-16 in Weber, K. T. (Ed.), Final Report: Detection Prediction, Impact, and Management of Invasive Plants Using GIS. 196 pp.

Griffin, D.W., C.A. Kellogg, and E.A. Shinn. 2001. Dust in the Wind: Long Range Transport of Dust in the Atmosphere and Its Implications for Global Public and Ecosystem Health. Global Change and Human Health 2(1): 20-33

Hunt Jr., E.R., J.H. Everitt, J.C. Ritchie, M.S. Moran, D.T. Booth, G.L. Anderson, P.E. Clark, and M.S. Seyfried 2003. Applications for Research using Remote Sensing for Rangeland Management. Photogrammetric Engineering and Remote Sensing 69(6):675-693

Ifarraguerri, A. and C. I. Chang. 2000. Unsupervised Hyperspectral Image Analysis with Projection Pursuit. IEEE Transactions on Geoscience and Remote Sensing. 38(6):2529-2538

Khanna, S., A. Palacios-Orueta, M. L. Whiting, S. L. Ustin, D. Riano, and J. Litago. 2007. Development of Angle Indexes for Soil Moisture Estimation, Dry Matter Detection, and Land-Cover Discrimination. Remote Sensing of Environment 109:154-165

Kincaid, D.R. and G. Williams. 1966. Rainfall Effects on Soil Surface Characteristics Following Range Improvement Treatments. Journal of Range Management 19:346-351

Kruse, F. A., Lefkoff, A. B., Boardman, J. B., Heidebrecht, K. B., Shapiro, A. T., Barloon, P. J., and Goetz, A. F. H., 1993. The Spectral Image Processing System (SIPS) - Interactive Visualization and Analysis of Imaging Spectrometer Data. Remote Sensing of Environment 44: 145 - 163

McMurtrey, J.E. III, E.W. Chappelle, C.S.T. Daughtry, and M.S. Kim. 1993. Fluorescence and Reflectance of Crop Residue and Soil. J. Soil Water Conserv. 48:207–213

Morgan, R.P.C. 1986. Soil Erosion and Conservation. Longman Scientific & Technical, Wiley, New York.

O'Brien, R.A., C.M. Johnson, A.M. Wilson, and V.C. Elsbernd. 2003. Indicators of Rangeland Health and Functionality in the Intermountain West. U.S. Department of Agriculture, Rocky Mountain Research Station. General Technical Report RMRS-GTR-104.

Okin, G. S. and M. C. Reheis. 2002. An ENSO Predictor of Dust Emission in the Southwestern United States. Geophysical Research Letters 29(9) 46 (1-3).

Palmer, A.R., and A. Fortescue. 2003. Remote Sensing and Change Detection in Rangelands. Proceedings of the VIIth International Rangelands Congress 675-680

Pellant, M. 1996. Use of Indicators to Qualitatively Assess Rangeland Health. Rangelands in a Sustainable Biosphere. Pages 434-435 *in* West, N. E. (Ed), Proc. Vth International Rangeland Congress. Society for Range Management. Denver, CO

Pyke, D.A., J.E. Herrick, P. Shaver, and M. Pellant. 2002. Rangeland Health Attributes and Indicators for Qualitative Assessment. Journal of Range Management 55:584–297

Roberts, D. A., J.B. Adams, and M.O. Smith, 1993. Discriminating Green Vegetation, Non-Photosynthetic Vegetation, and Soils in AVIRIS data. Remote Sensing of Environment. 44(2/3): 255–270

Savory, A. 1999. Holistic Management: A New Framework for Decision Making. Island Press. 616 pp

Settle J., and N. A. Drake, 1993. Linear Mixing and the Estimation of Ground Cover Proportions. International Journal of Remote Sensing, 14:1159–1177

Thome, K., B. Markham, J. Barker, P. Slater, and S. Biggar. 1997. Radiometric Calibration of Landsat. Photogrammetric Engineering and Remote Sensing. 63:856-858

Van Leeuwen, W. J. D., and Huete, A. R. 1996. Effects of Standing Litter on the Biophysical Interpretation of Plant Canopies with Spectral Indices. Remote Sensing of Environment. 55 123–138

Washington-Allen, R.A., N.E. West, R.D. Ramsey, and R.A. Efroymson. 2006. A Protocol for Retrospective Remote Sensing-Based Ecological Monitoring of Rangelands. Rangeland Ecological Management 59:19-29

Weber, K. T. 2006. Challenges of Integrating Geospatial Technologies into Rangeland Research and Management. Rangeland Ecology and Management 59:38-43

Whitford, W.G., A.G. De Soyza, J.W. Van Zee, J.E. Herrick, and K.M. Havstad. 1998. Vegetation, Soil, and Animal Indicators of Rangeland Health. Environmental Monitoring and Assessment 51:179-200

Williams, D. 1998. Landsat 7 Science Data Users Handbook. URL = http://landsathandbook.gsfc.nasa.gov/handbook/handbook_toc.html visited 7-November-2008

Williams, D. and W. Kepner. 2002. Imaging Spectroscopy for Determining Rangeland Stressors to Western Watersheds. U.S. Environmental Protection Agency technical reference EPA/600/R-01/004

Recommended citation style:
Weber, K.T., N.F. Glenn, J. Tibbitts, 2010. Investigation of Potential Bare Ground Modeling Techniques using Multispectral Satellite Imagery. Pages 101-112 in K. T. Weber and K. Davis (Eds.), Final Report: Forecasting Rangeland Condition with GIS in Southeastern Idaho (NNG06GD82G). 189 pp.